Chapter 2
Ultrasonic Synthesis of Functional Materials

Abstract Acoustic cavitation generates both physical and chemical effects. In this chapter, it has been discussed that some chemical reactions need the physical forces only where mass transfer effects are dominated. Some chemical reactions are caused primarily by the reactive radicals generated during acoustic cavitation. Reactions involving immiscible liquids, such as emulsion polymerisation process, need both the physical and chemical forces generated during acoustic cavitation process. Synthesis of functional inorganic, organic and biomaterials using ultrasound has been discussed in detail with specific examples. In addition, ultrasonic processing of food matrices to increase their functionality has also been included.

Keywords Ultrasound · Acoustic cavitation · Sonochemistry · Functional materials · Nanoparticles · Polymer latex · Synthesis of functional materials · Food processing · Core-shell materials

As mentioned in Chap. 1, the physical and chemical forces generated during acoustic cavitation could be used to synthesise a variety of functional materials. A functional material refers to an organic or inorganic material possessing specific functional properties. For example, some metal nanoparticles possess catalytic or antimicrobial properties [1, 2]; some metal oxides could be used in energy conversion applications [3–5]; some core-shell materials could be used for drug delivery applications [6–9]. The aim of this Brief is to provide a snapshot of the use of ultrasound in preparing functional materials with selected examples. A number of review articles [10–19] and edited books [20–24] are available on individual topics covered in this book that provide extensive literature review on various aspects discussed here.

2.1 Functional Inorganic Nanoparticles

Numerous studies have been carried out on synthesising metal and metal compound nanoparticles using acoustic cavitation process in organic and aqueous solutions. The fundamental mechanism involved in generating metal or metal compound

M. Ashokkumar, *Ultrasonic Synthesis of Functional Materials*,
SpringerBriefs in Green Chemistry for Sustainability,
DOI 10.1007/978-3-319-28974-8_2

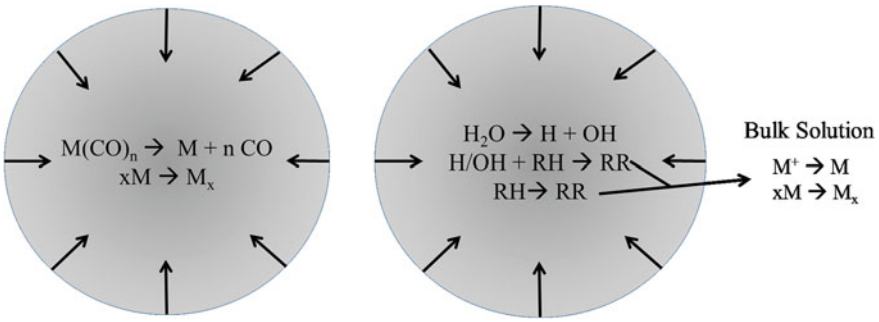

Fig. 2.1 Schematic representation of the formation metal nanoparticles (M_x): *Left* from metal carbonyl compounds (M(CO)n within the collapsing bubbles in an organic solvent; *Right* by the reduction of metal ions in aqueous solutions by reducing radicals (RR) generated within the bubbles. M—neutral metal atom; CO—carbon monoxide ligand; M^+—metal ion; RH—organic solute

nanoparticles is the heat generated within the cavitation bubbles. In organic liquids, volatile metal complexes are used to generate metal and metal oxides. In aqueous solutions, metal salts are used. These two methodologies have completely different mechanisms to produce functional nanoparticles, which are schematically shown in Fig. 2.1. The reaction sequence schematically shown in Fig. 2.1 also highlights the key events. Suslick and coworkers [13], Gedanken and coworkers [11] and other researchers [25] have used volatile coordination compounds containing zero valent metal atoms to generate metal nanoparticles.

When cavitation bubbles expands during the rarefaction cycle of the sound wave, volatile compounds evaporate into the bubble. In one example, $Fe(CO)_5$ dissolved in octanol diffused into the bubble and decomposed during bubble collapse due to high temperature conditions leading to the formation of Fe nanoparticles. Due to a high cooling rate (of the order of 10^9 K/s), the material generated was amorphous in nature and showed high catalytic activity compared to commercial samples [26].

It has been noted that the ultrasonically generated iron nanoparticles showed higher catalytic activity towards specific reactions. Suslick and coworkers [26] tested the catalytic activity of sonochemically synthesised iron particles for Fischer-Tropsch hydrogenation reaction and compared the activity with that of commercial samples. The efficiency of the sonochemically produced iron particles was about 2–5 times higher than that of the commercial samples.

In addition to making metal nanoparticles such as Fe [26], Co [27], Pd [28] and Ni [29], the method was also applied for synthesising carbon nanotubes and luminescent silica nanoparticles [30]. Authors have speculated that black carbon polymer could be produced under the extreme heat generated within the cavitation bubble by the decomposition of organic compounds followed by fast annealing process by the turbulent flow and shockwaves generated on bubble collapse. Sonochemical synthesis of nanostructured MoS_2 was achieved by the ultrasonic irradiation of

$Mo(CO)_6$ and sulphur in tetramethylbenzene, which were found to be excellent catalysts for thiophene hydrosulfuization [31].

Extensive work has been carried out on the sonochemical synthesis of metal and metal oxide nanoparticles in aqueous solutions. As mentioned earlier, the reaction mechanism is completely different to that observed in an organic medium. In the examples discussed above, the formation of metal nanoparticles occurs within the hot zone of the cavitation bubbles (Fig. 2.1). Whereas in aqueous solutions, the metal nanoparticles are generated either at the bubble/solution interface or in the bulk solution. As per Reaction 1 (Sect. 1.3), H atoms are generated, which could be used as a reducing agent. When an aqueous solution containing dissolved metal ions is sonicated, H atoms generated within the bubbles diffuse out into the bulk and react with metal ions to generate metal atoms (Reaction 9) which could agglomerate to form metal nanoparticles.

$$M^+ + \mathbf{H} \rightarrow M + H^+ \qquad \text{(Reaction 9)}$$

Henglein and coworkers [32] have cleverly used a small amount of volatile organics (simple alcohols, RHOH) to capture the primary radicals to generate relatively large amount of secondary reducing radicals (Reaction 10), a technique commonly used in radiation chemistry.

$$\mathbf{H/OH} + \mathrm{RHOH} \rightarrow \mathbf{ROH} + H_2/H_2O \qquad \text{(Reaction 10)}$$

ROH radicals (alcohol radicals), strong reducing agents, react with metal ions to generate metal atoms which then agglomerate to form metal nanoparticles (Reactions 11 and 12). It is also known that alcohol or other volatile organic molecules that diffuse into the cavitation bubbles get pyrolysed within the bubbles and generate a variety of reducing radicals (**R**), which could also be involved in the reduction reaction (11).

$$\mathbf{ROH} + M_+ \rightarrow M + \text{Other products} \qquad \text{(Reaction 11)}$$

$$nM \rightarrow M_n \qquad \text{(Reaction 12)}$$

Okitsu et al. [33–35] and Grieser and coworkers [36–39] have carried out extensive research work on the sonochemical synthesis of metal and metal compound nanoparticles in aqueous medium. Most of their studies focussed upon controlling the size, size distribution and shape of the nanoparticles by manipulating various experimental parameters. One of the key findings of these investigations is the correlation between the rate of radical formation and the size and size distribution of the metal nanoparticles [35]. As discussed in Chap. 1, the amount of primary and secondary radicals generated during acoustic cavitation depends on the operating frequency when other experimental parameters are kept unchanged. As discussed in Sect. 1.3, the amount of primary radicals generated during acoustic cavitation is very low at 20 kHz, increases with an increase in frequency and then decreases beyond a certain frequency. The rate of gold formation is found to increase with an increase in frequency initially followed by a decrease at very high frequencies (Fig. 2.2).

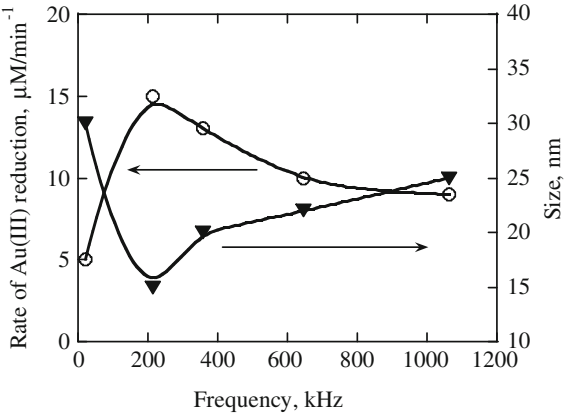

Fig. 2.2 Rate of Au(III) reduction and the corresponding size of Au nanoparticles as a function of ultrasound frequency (Adapted from Ref. [35])

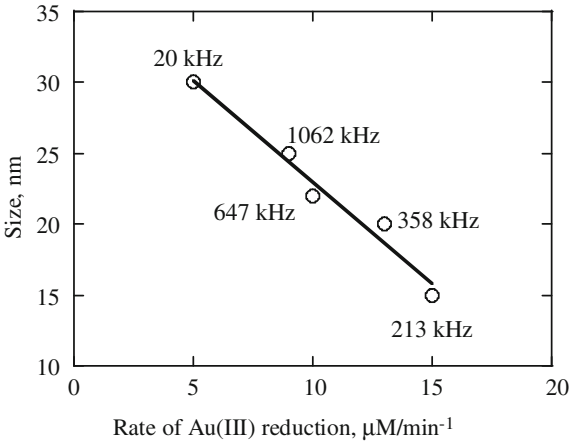

Fig. 2.3 Size of Au nanoparticles generated in relation to rate of Au(III) reduction at various frequencies. Adapted from Ref. [35]

This trend correlates well with that of primary radical formation. In the same work, Okitsu et al. [35] also measured the size and size distribution of Au nanoparticles and found that the average size of Au nanoparticles decreased with an increase in frequency initially and increased at very high frequencies—a similar trend to that of primary radicals and rate of Au formation. Further analysis of the data showed that it is not the acoustic frequency that controls the average size of the particles but the rate of Au(III) reduction.

It can be seen in Fig. 2.3 that the size has a linear relationship with the rate of reduction, which in turns depends upon the amount of reducing radicals generated at various frequencies. This is an important finding since it reinstates the general principles with regard to particle size control. When crystals are produced, two processes control the size, namely nucleation and growth. If the rate of nucleation is faster than the rate of growth, then smaller particles are produced and vice versa.

The observation in Okitsu et al.'s study [35], higher the rate of radical formation smaller the particle size, indicates that the general principles of crystal formation and growth are valid under sonochemical synthetic conditions.

A second aspect that is of interest in sonochemical synthesis of metal nanoparticles is the formation of core-shell bimetallic particles. Vinodgopal et al. [40] have tried to synthesise Pt-Ru bimetallic alloy particles aiming at using them in methanol oxidation fuel cells. It is known that CO-poisoning lowers the efficiency of fuel cells when Pt is used an electrode material. The use of Ru-Pt alloy would prevent CO-poisoning. However, when a mixture of Pt and Ru salts was sonicated in aqueous solutions, Pt-core-Ru-shell nanoparticles in the size range 2–20 nm were formed (Fig. 2.4a). The issue here is the relative ease of the reduction of Pt ions compared to the reduction of Ru. The Pt nanoparticles are first produced by the sonochemically generated reducing radicals, which then act as electron pools to reduce Ru(III) ions. Ru(III) ions are reduced on the surface of Pt nanoparticles forming a shell around them. Vinodgopal et al. have also successfully generated Ru-Pt alloy nanoparticles using PVP as the stabiliser. The prepared alloy nanoparticles were tested for their catalytic efficiency in methanol oxidation fuel cells. This work was later followed by Anandan et al. to make Au-Ag [41] and Au-Ru [42] core shell particles, in order to demonstrate the versatility of this methodology.

Exfoliated graphene sheets have found applications in fuel cells and sensors. Functionalised reduced graphene oxide (RGO) nanoparticles were sonochemically synthesised by Vinodgopal et al. [43]. High frequency sonication (211 kHz) of an aqueous solution containing GO, gold chloride and PEG resulted in the simultaneous reduction of GO to RGO and deposition of gold nanoparticles on the surface of RGO sheets (Fig. 2.5). In a follow up study, the authors have used a dual frequency approach to generate exfoliated RGO-Pt nanocomposites with better efficiency towards methanol oxidation process [44]. In this case, the strong physical forces generated by 20 kHz ultrasound was used for the exfoliation of GO and the high frequency ultrasound was used to achieve reduction reactions necessary for the generation of RGO-Pt nanocomposites.

Neppolian et al. [45] have further developed this process for synthesising Pt-Pd bimetallic particles loaded RGO nanosheets for methanol oxidation fuel cells. These composite particles showed very high electrocatalytic activity. In particular, this study focused on varying the molar ratio of Pt/Pd bimetallic particles on the catalytic activity. They have observed that 1:1 Pt/Pd-loaded RGO showed optimal electrocatalytic activity with a minimum onset potential and maximum current density.

It could be seen from the discussion provided so far in this chapter that sonochemical synthesis of functionalised nanomaterials show superior catalytic properties demonstrating the versatility of this methodology. In particular, the sonochemical method generates very small nanoparticles in the size range 2–10 nm, which is normally difficult to be generated by chemical methods in aqueous medium. Another advantage here is the in situ generation of the metal nanoparticles for loading onto other surfaces.

In addition to catalytic properties, the sonochemically synthesised metal nanoparticles have also been found useful in biomedical applications. It has been shown

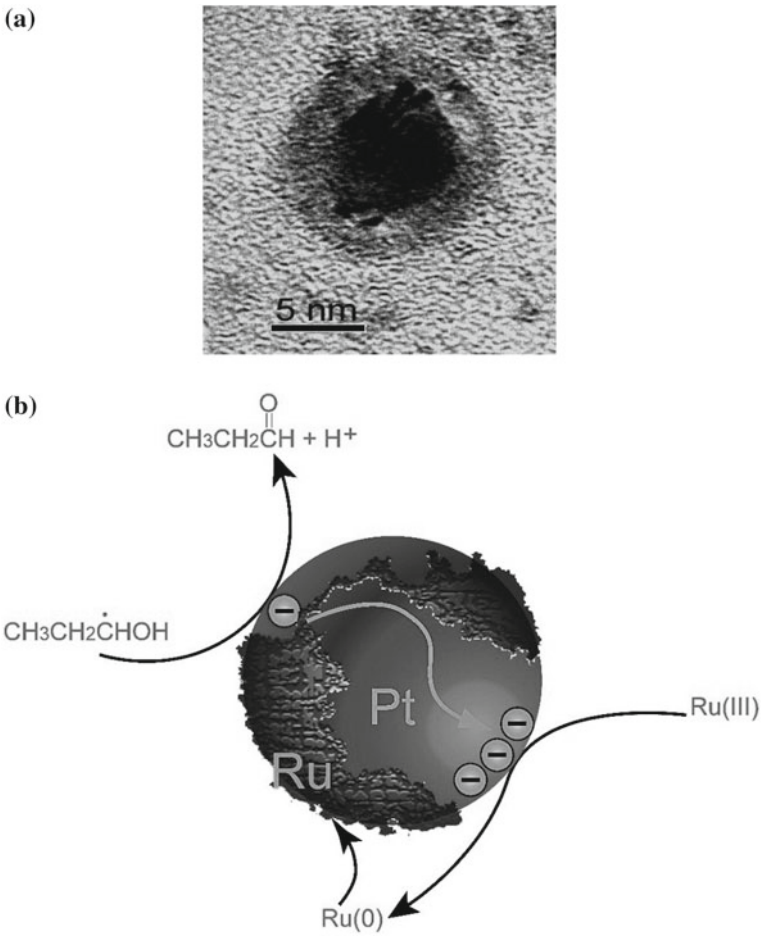

Fig. 2.4 **a** Pt-Ru core-shell nanoparticles generated by the sonochemical reduction of Pt and Ru ions in aqueous solutions at 211 kHz; **b** Schematic representation showing the formation of Pt core followed by Ru shell. Adapted from Ref. [40]

that sonochemically synthesised gold nanoparticles could be used in biosensing [46]. The gold nanoparticles seem to electronically interact with Adenine Thymine-DNA (AT-DNA) and Guanine Cytosine-DNA (GC-DNA). Such interactions could be monitored by the photoluminescence properties of the biomolecules.

TiO_2 has been used as a photocatalyst in numerous studies [47–49]. The photocatalytic properties of TiO_2 strongly depend upon the method of preparation and hence numerous investigations have focused on establishing a relationship between the functional properties of TiO_2 and the method of preparation [50–54]. Ultrasonic methodology has been extensively used in the preparation of TiO_2 nanoparticles in various forms [55–58]. In addition to TiO_2, other metal oxide nanocomposites have

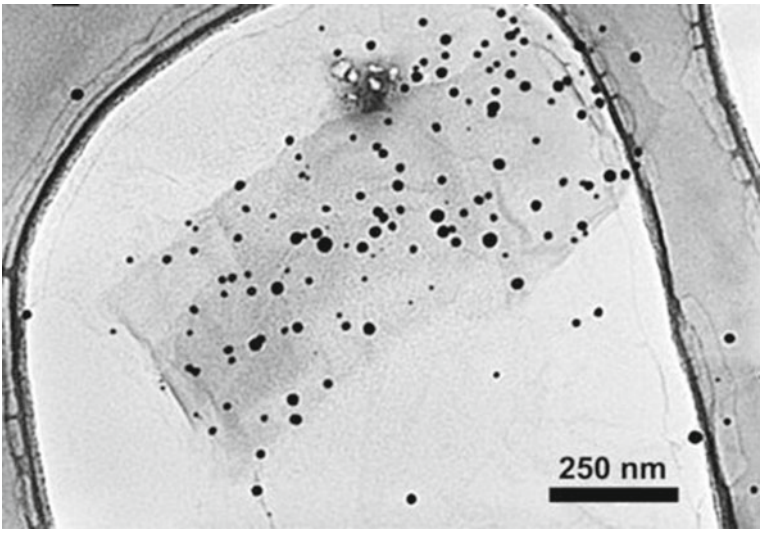

Fig. 2.5 TEM micrograph of the RGO-Au composite prepared by the sonochemical reduction of GO and Au(III) ions using 211 kHz. Adapted from Ref. [43]

also been synthesised using ultrasonic methodology. For example, the sonication of a solution containing a mixture of copper(II) acetate and bismuth(III) nitrate in the presence of sodium hydroxide and polyvinylpyrrolidone (stabilizing agent) has led to the formation of Bi_2CuO_4 nanoparticles possessing flake-like morphology [59]. The formation of such unusual morphologies is due to the unique and extreme experimental conditions generated during acoustic cavitation. These nanostructured composite materials have been found to possess high photocatalytic activity compared to individual oxides (CuO and Bi_2O_3).

One of the major issues in using nanoparticles for the degradation of organic pollutants in aqueous environment is the removability of these materials after processing. Due to their very fine size, filtration of the photocatalytic nanoparticles from aqueous solution is a difficult and energy intensity process. For this reason, there is significant interest from both research and industrial communities for synthesising micron sized catalytic particles possessing nanoporos structures. The nanoporosity would provide the advantage of high surface area required for a high photocatalytic efficiency and the micron size would help for easy removal from the solution following the catalytic process.

Zhou et al. [60] have recently developed a novel methodology to synthesise nanoporos TiO_2 microspheres. It involved the dispersion of either hydrophilic TiO_2 particles in an aqueous chitosan solution or hydrophobic TiO_2 particles in an organic solvent layered on an aqueous chitosan solution followed by sonication using a 20 kHz horn. As shown in Fig. 2.6, porous TiO_2-shelled microspheres or TiO_2-rich core microspheres could be prepared by choosing appropriate experimental

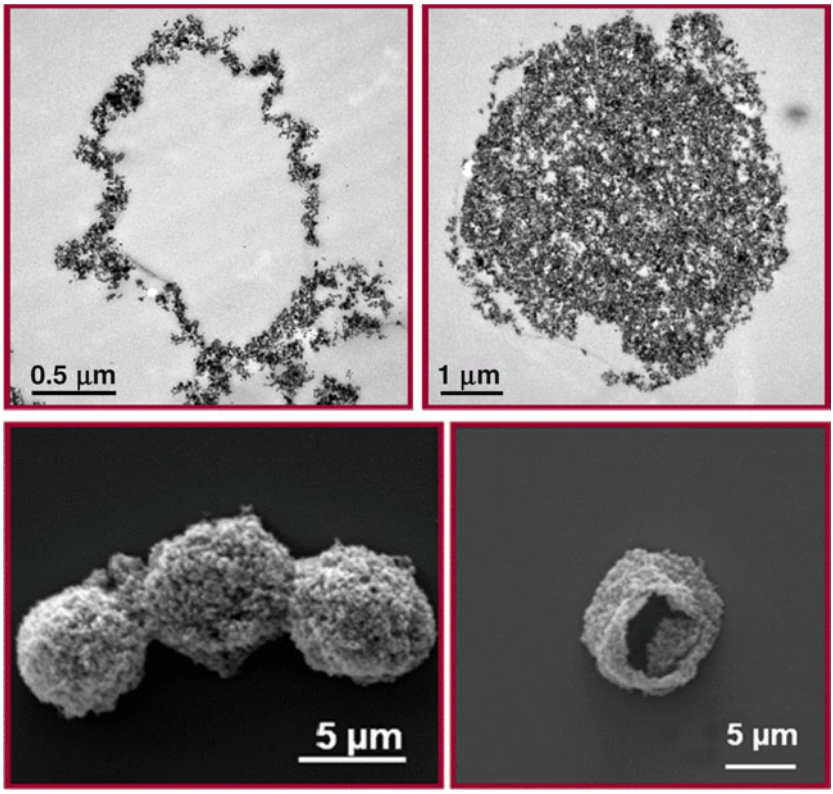

Fig. 2.6 *Top* Cross-sectional TEM images of *Left* TiO_2-rich-shell-loaded chitosan microspheres [60]; *Top Right* TiO_2-rich-core-loaded chitosan microspheres; *Bottom* SEM images of *Left* Chitosan microspheres before calcination and *Right* TiO_2 hollow/porous microspheres after calcination

conditions. The procedure involved calcination of chitosan which was used to form the microsphere skeleton. A detailed mechanism for the formation of these microspheres with two different morphology has been discussed.

In order to demonstrate the functionality of the TiO_2 microspheres, their antimicrobial property was studied using growth of E. coli as a model system. The growth of E. coli was completely inhibited by TiO_2 microspheres up to 24 h compared to a control. TiO_2 microspheres containing nanoporos structures have shown similar photocatalytic activity compared to Degussa TiO_2 nanoparticles with added advantage of easy removability. This study has established the fact that ultrasonic method could be used to prepare density controlled porous catalytic materials for a variety of potential industrial applications that include paints possessing antimicrobial properties, adsorption of dyes from industrial effluents, drug encapsulation and delivery, etc.

2.2 Functional Organic Nanoparticles

Ultrasonic/sonochemical synthesis of polymer latex particles has shown several advantages over conventional polymerisation process [61]. Enhanced rate, particle size control, polymerization in the absence of an initiator, high and uniform molecular weight distribution and low temperature polymerisation process are some advantages that could be highlighted. The mechanism of ultrasonic polymerisation process involves both the physical and chemical forces generated during acoustic cavitation. Initially, the shear forces and interfacial capillary forces generated help generate nanometre sized monomer emulsion droplets in aqueous phase. The primary and secondary radicals generated within cavitation bubbles diffuse into monomer droplets initiating polymerisation thus converting each monomer droplet into a polymer particle. These events are schematically represented in Fig. 2.7. Often surfactants are used to stabilise monomer droplets.

The reaction mechanism of ultrasonic polymerisation has been elucidated by Bradley and Grieser [62]. They have suggested that the initial reaction step is the reaction between the primary radicals generated in Reaction 1 and monomer molecules to generate monomer radicals (**MR**; Reaction 13) in the aqueous phase. These radicals then enter into a monomer droplet (MD; Reaction 14) and initiate the

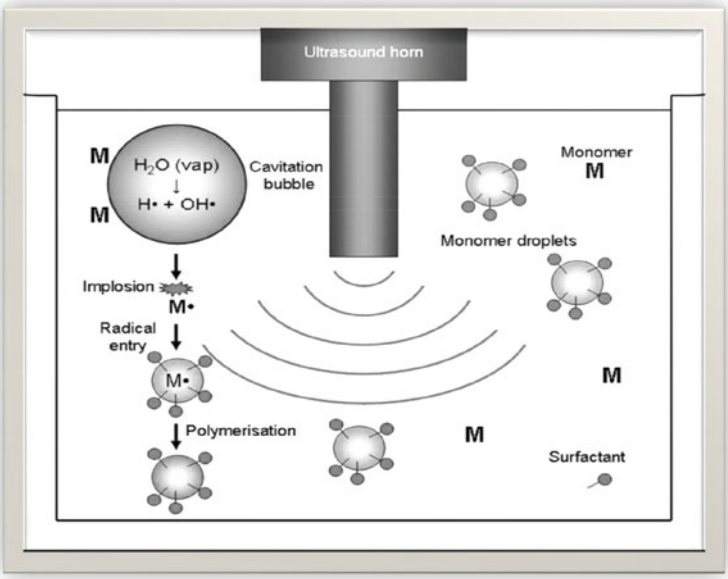

Fig. 2.7 Acoustic cavitation-induced polymerisation of a monomer to generate polymer latex particles using 20 kHz ultrasonic horn [61]. The shear forces generates emulsion droplets. Radicals generated within cavitation bubbles react with monomer molecules to generate monomer radicals that diffuse into monomer droplets to initiate polymerisation process

polymerisation (propagation) reaction (14). Termination of the polymerisation process occurs when growing radicals (PC(i) and PC(ii)) react among themselves as shown in Reaction 15. Detailed kinetic models for ultrasonic polymerisation reactions are available in the literature [63, 64].

$$\mathbf{H/OH} + \mathrm{M} \rightarrow \mathbf{MR} + \mathrm{H_2/H_2O} \qquad \text{(Reaction 13)}$$

$$\mathbf{MR} + \mathrm{MD} \rightarrow \mathbf{PC(i)} + \mathbf{PC(ii)} \qquad \text{(Reaction 14)}$$

$$\mathbf{PC(i)} + \mathbf{PC(ii)} \rightarrow \mathrm{PF} \qquad \text{(Reaction 15)}$$

Most of the ultrasonic polymerisation studies involve miniemulsion polymerisation process where both shear and radicals generated by acoustic cavitation at 20 kHz are important. However, Teo et al. [65] have also used high frequency (213 kHz) to successfully carry out microemulsion polymerisation. By manipulating the concentration of surfactant used to stabilise the emulsion droplets, shear forces needed to generate emulsion droplets could be avoided.

Teo et al. [66] have developed a novel methodology to control the molecular weight of polymers generated by ultrasonic emulsion polymerisation process. In this procedure, an organic solvent was mixed with the monomer in different proportions. When various amounts of toluene were mixed with the monomer, the rate of polymerisation decreased with an increase in the amount of toluene. This is due to the formation of donor/acceptor complex between propagating monomer/polymeric radical and toluene molecules slowing down the propagation rate. A number of aromatic organic liquids (halobenzenes and xylene) showed similar effects. What is interesting is that when aliphatic organic liquids were used, no such effect of retarding rate of polymerisation was observed. Hence, the presence of an aromatic ring is important for the formation of the complex mentioned above. Another interesting observation in this study is that the molecular weight of the polymer was influenced by the presence of both aromatic and aliphatic organic liquids. Teo et al. [66] have related the change in molecular weight to chain transfer constant which could be obtained by plotting 1/DP (degree of polymerisation) against the ratio between organic liquid and monomer amounts.

They have also synthesised thermoresponsive [67] and magnetised [68] polymer latex particles. For the later, butylmethacrylate (BMA) monomer containing presynthesised magnetite nanoparticles of 10 nm in size was ultrasonically emulsified in an aqueous surfactant solution. The subsequent formation of poly-BMA latex particles resulted in the homogeneous incorporation of magnetic particles within the latex particles. The colloidal solution containing magnetite-loaded poly-BMA showed strong magnetic activity (Fig. 2.8).

The supramagentic properties of magnetite-loaded poly(BMA) particles were evaluated using vibrating sample magnetometry technique. It has been suggested that the one-pot synthetic methodology could be used to synthesise such functional composite materials for potential applications in separation technologies and encapsulation and controlled release of drugs and food flavours.

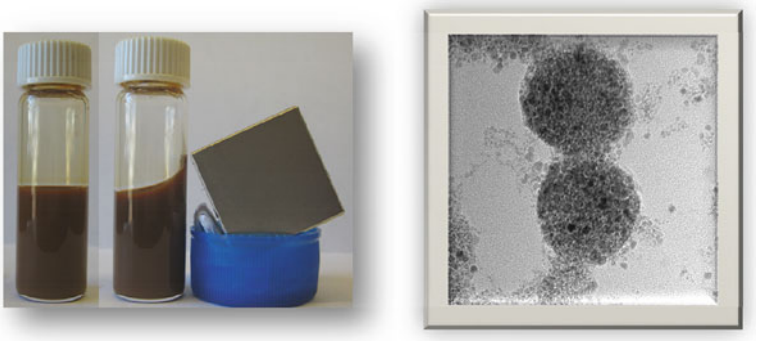

Fig. 2.8 *Left* Photograph showing the magnetic properties of magnetite-loaded poly(BMA) latex particles; *Right* TEM image showing the magnetite-loaded poly(BMA) latex particle. Adapted from Ref. [68]

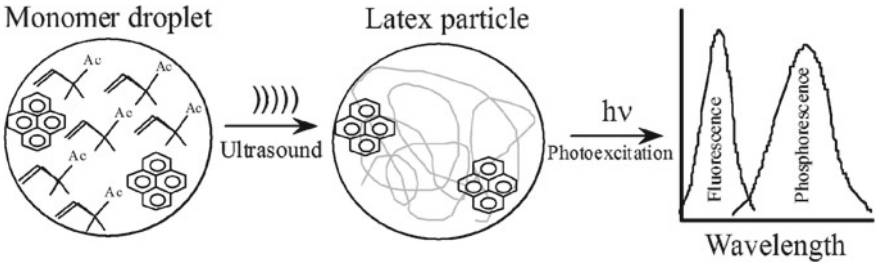

Fig. 2.9 Schematic diagram showing the incorporation of pyrene into MMA monomer droplet resulting in the incorporation of the fluorescence solute into the latex particles that makes the latex particle with fluorescence properties [69]

Bradley et al. [69] have extended the sonochemical polymer latex formation technique to synthesise fluorescent and phosphorescent latex particles. The method, schematically shown in Fig. 2.9, simply involved the ultrasonic emulsification of methylmethacrylate monomer in an aqueous surfactant solution where a fluorescence or phosphorescent solute was pre-dissolved in the monomer phase. When pyrene was used as a fluorescent solute, the dielectric constant of the latex particles could be evaluated. Due to the incorporation of the fluorescence solutes into the polymer latex matrix, the interaction between excited state and ground state monomer could be avoided resulting in the lack of dimer emission and domination of monomer emission.

Using the ratio between band intensities of pyrene emission at specific wavelengths, the dielectric constant of the latex could be evaluated. Phosphorescent poly-MMA particles were also produced using 1-bromonaphthalene.

Atobe and coworkers [70, 71] have used Tandem acoustic technique to make transparent emulsions and extended this technique to synthesise latex particles with

controlled size range. The synthesis of size controlled polymer nanoparticles involved the sonication of monomer aqueous solution at 20 kHz followed sequentially by 500 kHz, 1.6 and 2.4 MHz—such procedure generated emulsion droplets of 103 nm after 20 kHz sonication, then 87, 61 and 47 nm, respectively. Such monomer droplets were found very stable in the absence of any surfactant. The addition of a chemical initiator to the transparent emulsions initiated polymerisation reaction converting the monomer droplets to polymer particles without significant changes to their size range.

2.3 Functional Microspheres

Encapsulation and delivery of drugs and nutritional compounds is an active area of research. In general, most functional compounds such as drugs and nutrients are nonpolar and hence delivery in the form of aqueous solution is an issue. Conventional emulsification techniques such as homogenisation including ultrasonic homogenisation is used to prepare an emulsion of the functional compound, protected by emulsifiers using surface active agents. However, such emulsions are not stable and long-term storage is an issue. Protein/lipid/carbohydrate-shelled microspheres encapsulating air or other functional materials have been found useful in numerous applications involving encapsulation and delivery. Suslick and coworkers [72, 73] used ultrasonic technology to prepare air-filled protein microspheres that could be used as ultrasound contrast agents. The process not only generated protein-coated air-filled microspheres but also formed a strong protein shell due to cross-linking of proteins by cavitation generated radicals. The process involved is schematically shown in Fig. 2.10 [74].

Typically, an aqueous solution containing 5% BSA (bovine serum albumin) is sonicated at 20 kHz using a horn-type sonicator at relatively high acoustic power

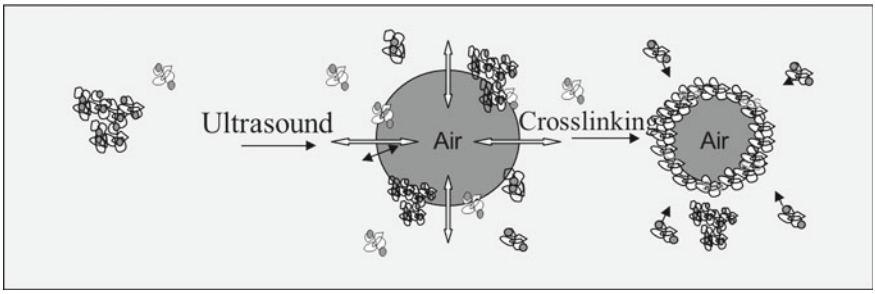

Fig. 2.10 Schematic representation of air-filled microsphere formation in an ultrasonic field. Partially denatured protein molecules adsorb at the ultrasonically-generated bubble solution interface. Superoxide radicals generated during acoustic cavitation leads to inter-molecular cross-linking of proteins resulting in the formation of stable protein-shelled microbubbles [74]

levels. There are a few key steps involved in this process. First, partial denaturation of the protein should be carried out to increase the surface activity of the protein. In its natural globular state, the surface activity of these proteins is low. Proteins in their natural state have globular structure held together by intramolecular forces such as disulphide bonds or hydrophobic interactions. Partial denaturation could be achieved either thermally or by chemical means [72–74]. Such partial denaturation of proteins leads to aggregation followed by adsorption at bubble/solution interface. The positioning of the horn is also important in this process. If air is to be encapsulated, the tip of the horn should be positioned at air/solution interface. If an organic liquid (or functional liquid material) needs to be encapsulated, the tip of the horn should be positioned at organic liquid/aqueous solution interface. Figure 2.11 shows SEM images of liquid-filled microspheres.

While the above-mentioned procedure is similar to conventional emulsification process, ultrasonic technology leads to the cross-linking of the proteins to form a stable shell around air or liquid core. The partial denaturation process in general breaks inter-molecular disulphide bonds present in the protein leading to the formation of free thiols. As mentioned earlier (Reaction 5), $\mathbf{HO_2}$ radicals are generated during acoustic cavitation in air-saturated aqueous solutions, which are used to generate inter-molecular disulphide bonds between protein molecules adsorbed at the bubble or liquid droplet surface. Such cross-linking provides strength to the shell making the microspheres very stable [74].

While inter-protein molecular disulphide bonds are shown to strengthen the shell, Gedanken and coworkers [75] have used proteins that do not possess –SH functional groups. Using streptavidin and avidin as the shell materials, they prepared functional microspheres. A recent work by Cavalieri et al. [76] has performed a systematic study on the importance of cross-linkable functional groups in order to produce stable microspheres. They prepared poly(methacrylic acid) (PMA) containing different degree of –SH moieties (0, 5, 10 and 30 %). Using PMA and PMASH, microspheres were ultrasonically prepared and characterised. It was found out that microbubbles made of pure PMA and 5 % –SH were not stable whereas PMASH microbubbles containing >10 % –SH were found to be very stable. It was also found out that the

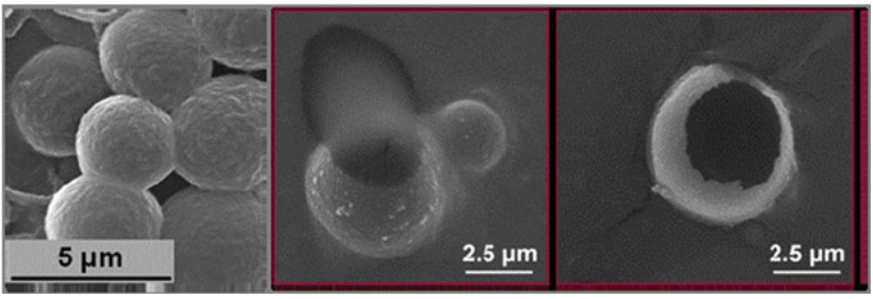

Fig. 2.11 SEM images of lysozyme microspheres (*left*), encapsulated liquid flowing from a broken microsphere (*middle*) and hollow shell (*right*) following liquid removal

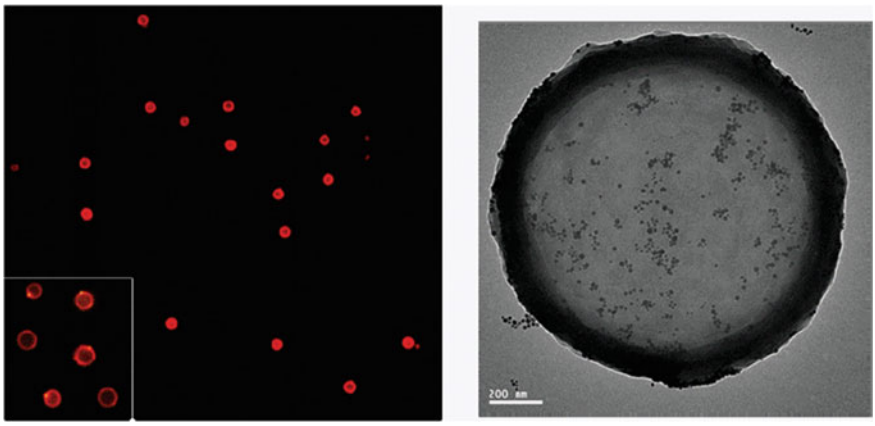

Fig. 2.12 *Left* PMASH microcapsules and microbubbles loaded with doxorubicin for drug delivery applications [76]; *Right* TEM image of gold nanoparticles-loaded lysozyme microbubbles used as a biosensor [77]

physical and functional properties of PMASH microspheres depended upon degree of thiolation. For example, the size of microbubbles almost doubled (8 μm) when 30 % –SH was present compared to those produced with 10 %. In addition, the surface morphology was found to be smoother with a thin shell when 10 % –SH was used whereas a rough and thicker shell was observed when 30 % –SH was used. The authors have also bio-functionalised these PMASH microcapsules and microspheres using doxorubicin and demonstrated their usefulness as targeted drug delivery vehicles (Fig. 2.12). The biofunctionality of lysozyme microbubbles has also been extended in a follow up study [77] that involved loading of gold nanoparticles on PMASH microsphere shell. In this case, the gold nanoparticles-loaded microbubbles showed a higher efficiency in biosensing applications.

Using phantom as a tissue mimicking structure, ultrasound backscattering capacity of gold nanoparticles-loaded lysozyme microbubbles (Fig. 2.12) was demonstrated. In addition, alkaline phosphate conjugated lysozyme microbubbles were shown to possess biosensing capabilities to detect small quantities of paraoxon.

Melino et al. [78] carried out further work to demonstrate the viability of using protein microspheres for drug, gene and nucleic acid delivery. One of the important factors that determines the potential viability of using any drug delivery vehicle is its biodegradability following delivery of drugs. In particular, partial denaturation of lysozyme during microsphere preparation may lead to protein aggregation and hence amyloid fibrils formation that is known to cause Alzheimer's disease. For this reason, the biodegradability of lysozyme microbubbles was evaluated using limited proteolysis using trypsin and the observed results are schematically shown in Fig. 2.13.

Using SDS-Page and HPLC, this study showed the fragmentation of lysozyme protein from the microbubble shell. As a control experiment, denatured lysozyme

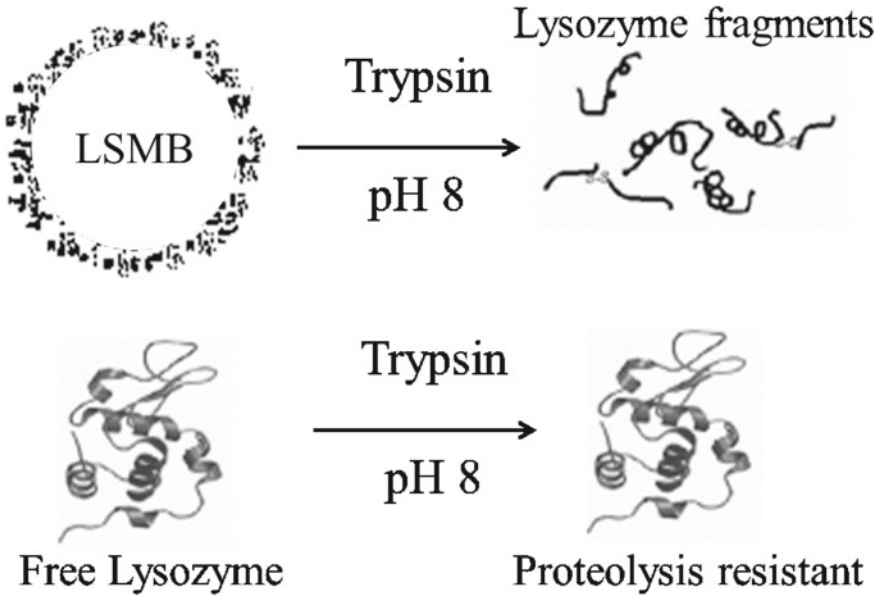

Fig. 2.13 Digestion of lysozyme from microbubble surface (LSMB) by proteolysis in the presence of Trypsin. Native lysozyme is resistant to proteolysis. Adapted from Ref. [78]

formed by heat was found to be resistant to trypsin proteolysis. In the same work, Melino et al. [78] have also demonstrated the capacity of lysozyme microbubbles to carry other functional biomolecules such as lactoferrin, DNA and dextran.

In all applications where protein microbubbles are used, the control over the size, size-distribution and stability (shell thickness) are crucial factors. Detailed investigations have been carried out on controlling such properties under varying experimental conditions. It has been shown that ultrasonic power, post-sonication procedure, duration of sonication, etc. have significant control over the physical properties of microbubbles. One novel finding reported recently [79] was the control of size and size distribution of protein microspheres by tuning the properties of the ultrasonic horn. It has been shown in this study that there is a strong correlation between active cavitation zone and the size distribution of microspheres. In this work, lysozyme microspheres were prepared using ultrasonic horns of varying tip length and also using a flow-through horn as shown in Figs. 2.14 and 2.15.

The size distribution of microspheres obtained using these horns are also shown in this figure.

It could be seen in that there is a direct correlation between diameter of the horn tip and size/size distribution of the microspheres. Smaller the horn tip diameter narrower the size distribution and smaller the average size of microspheres. In order to understand the mechanism for such a correlation, the active cavitation zone was analysed for these systems using sonochemiluminescence images (Fig. 2.15).

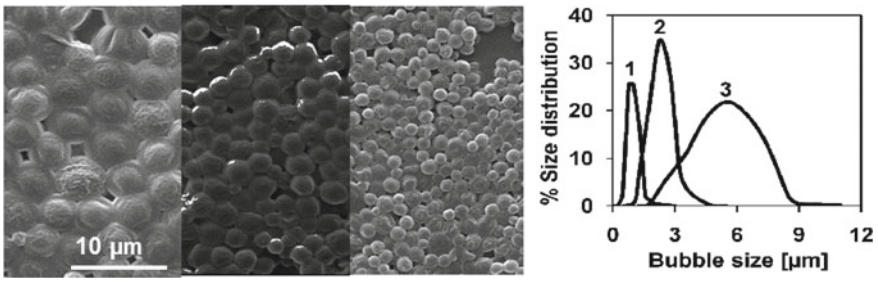

Fig. 2.14 SEM images showing lysozyme microspheres prepared using *Left* 1 cm tip, *Middle* 3 mm tip and *Right* flowthrough horns. The corresponding size distributions are shown in the plot. *1*: Flowthrough horn; *2*: 3 mm tip and *3*: 1 cm tip. Adapted from Ref. [79]

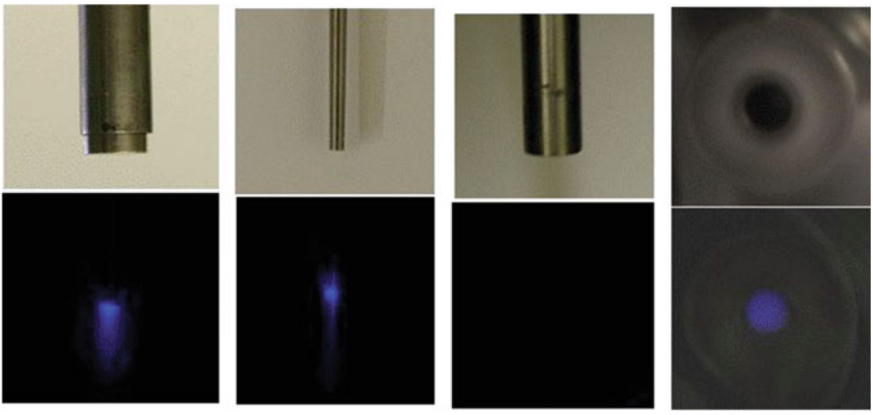

Fig. 2.15 *Top* Photographs of side views of 1 cm, 3 mm and flowthrough horns. The last image is a view from the bottom showing the hole in flowthrough horn. *Bottom* Corresponding SCL images showing active cavitation zones. Of interest is the absence of an active cavitation zone from side view for the flowthrough horn. Only two-dimensional active zone could be observed when viewed from the bottom. Adapted from Ref. [79]

It could be seen that the size/volume of active cavitation zone decreases with a decrease in the diameter of horn tip. Using these observations, the authors speculated that the physical effects generated during acoustic cavitation are more homogeneous when the cavitation zone is narrower, which leads to the formation of smaller microspheres with a narrow size distribution. The reason for the formation of very narrow sized nanospheres when a flow through horn was used is speculated to be due to the 2-dimensionaly active cavitation zone.

Recent work on starch-based microspheres [60], as discussed earlier, suggests that ultrasonic preparation procedure is a versatile method that could be used for the preparation of microspheres with a variety of shell and core materials. Chitosan

microspheres encapsulating organic liquids also paves a pathway to prepare targeted drug delivery vehicles.

2.4 Functional Foods

Delivering nutritional food has positive impacts on human health. Food industries have been focusing on making functional foods to improve their nutritional benefits and quality. Various technologies such as high pressure processing, high shear homogenisers, etc. are in used in food processing. In recent years, the use of ultrasound technology in food processing has been explored [80, 81]. While most of these studies look into extraction of nutraceuticals and high value compounds such as vitamins, a few have focussed on modifying the functional properties and synthesis of functionalised foods [22, 80, 81].

Food emulsions are traditionally used to incorporate nutraceuticals in complex food matrix. Ultrasonic dispersion of omega-3 oils in milk and juice has been reported recently. Conventionally, homogenisers have been used for this purpose. However, food emulsions generated using homogenisers are relatively less stable. Shanmugam and Ashokkumar [82] have used 20 kHz ultrasound to generate stable flaxseed oil emulsions in skim milk with a loading of up to 21 %. The key advantage of ultrasonic emulsification process in a milk system is that there is no need for the addition of external stabilisers. The physical forces generated during acoustic cavitation lead to partial denaturation of about 1 % of milk proteins, which act as stabilisers of the emulsion droplets. The emulsions generated were found to be stable for at least 9 days. Flaxseed oil emulsions in carrot juice was also successfully prepared [83] ultrasonically with a loading of about 1 %. It should be noted that FDA's GRAS notification number GRN000256 has indicated the level of use of high linolenic acid flaxseed oil in processed fruit/vegetable juices which should not exceed 0.9 %.

Homogenisation of milk using the physical forces generated during acoustic cavitation has been studied extensively [84]. It has been shown that sonication at 20 kHz has led to the reduction of fat globule sizes in milk, much smaller than that could be achieved by conventional homogenisers. It has been suggested that the shear forces generated by acoustic cavitation are responsible for the reduction in the size of fat globules in milk (Fig. 2.16).

It should be noted that ultrasonic technology is a non-thermal process and hence very little changes to the physical and functional properties of dairy system is observed due to sonication. In most studies, the processing time required is a few seconds to less than a minute. In order to evaluate the effect of sonication on the constituents of milk, Chandrapala et al. [85] and Shanmugam et al. [86] carried out extensive research in recent years. Their studies have shown that sonication of a dairy system causes very little changes to the physical properties of whey proteins. They observed reversible changes to partial denaturation of whey proteins. In order to see the effect, the constituents of whey proteins, namely, pure- and 3:1 mixtures of β-Lactoglobulin (β-LG) and α-Lactalbumin (α-LA)

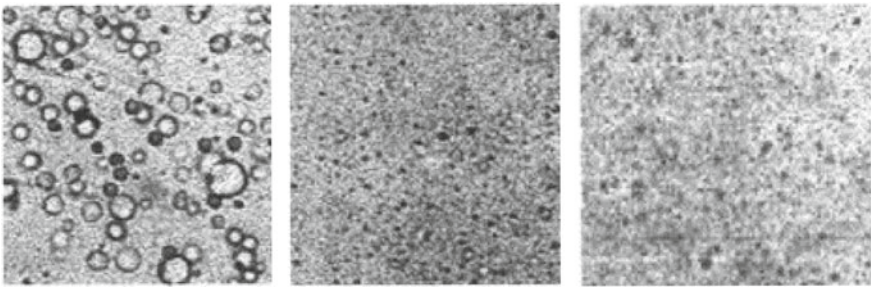

Fig. 2.16 Micrographs of milk samples, *Left* non-homogenised; Middle: homogenised and Right: sonicated (20 kHz). Average sizes of fat globules are ~5 μm, ~2 μm and ~1 μm for non-homogenised, homogenised and sonicated samples, respectively. Adapted from Ref. [84]

were sonicated up to 60 min [85]. They observed an increase in surface hydrophobicity and free thiol as a function of sonication. Therese changes were found to be reversible on storage overnight. The secondary structure of the proteins was not significantly affected.

Ashokkumar and coworkers [85–93] have also looked at the functional properties of various dairy and starch systems following sonication. They have shown that gels made of sonicated whey proteins showed better functional properties in terms of gel strength and syneresis. As mentioned earlier, sonication leads to partial denaturation of whey proteins. When heat-induced gelation process is applied on sonicated whey protein systems, a better gel network is produced leading to firmer gels. Due to the stronger protein network, the water holding capacity is found to be significantly higher for the sonicated samples, which refers to reduced syneresis. Both these properties are important for developing commercial products such as yoghurts and smoothies.

Another important functionality improvement that was achieved in dairy systems is heat stability of dairy proteins [87]. It is well-known that heat-induced aggregation of dairy proteins is one of the major issues in dairy industry when spray-dried milk powders are produced. Heating of high protein content solutions prior to spray drying leads to a significant increase in viscosity, sometimes leading to formation of a gel. This is highly undesirable in a processing plant which reduces production efficiency and increases cost in dairy industry. A simple solution to overcome this issue has been developed using ultrasonic processing technology. It can be seen in Fig. 2.17 that heating of whey protein solution leads to a significant increase in solution viscosity. This is due to the formation of protein aggregates by denatured whey proteins. Sonication of these aggregates reduced the viscosity back to the starting level. No more than a maximum sonication of 1 min was required to bring down the viscosity to almost initial level. This is important for an industrial process to minimise the energy requirement, if it to be adopted by dairy industry. What is more interesting and important is the post-heating effect on these samples. If the non-sonicated sample is heated further, viscosity increases significantly (Fig. 2.17).

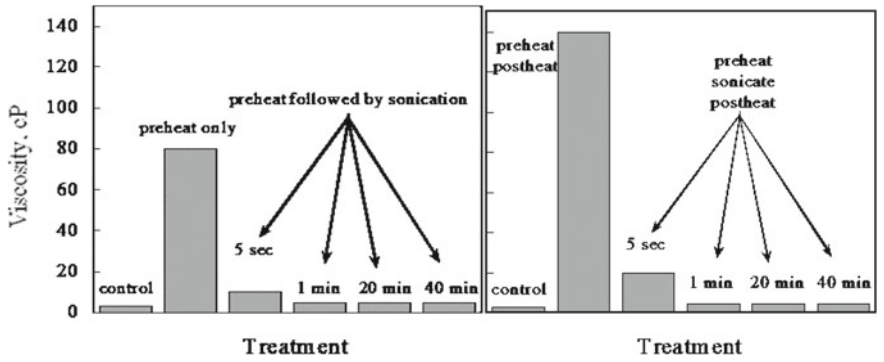

Fig. 2.17 Effect of sonication (20 kHz) on the viscosity of preheated WPC (9 % aqueous solution). The viscosity of sonicated samples remains unchanged following post heating. Adapted from Ref. [87]

However, post-heating of the sonicated samples did not increase the viscosity suggesting that the protein system was heat stable, which is what dairy industry needed.

Follow up work on similar systems including skim milk, high protein content solution, etc. provided further support to the claim that sonication could lead to improved functionality in terms of heat stability of dairy systems. Extending the work from lab scale to a pilot scale study [90], it has been shown that sonication is a viable technology for improving the heat stability of dairy proteins in dairy processing industry. To further support this process, Chandrapala et al. [91] also looked at the functionality of whey protein powders prepared by spray drying after sonication. The whey powder was stored for some days and reconstituted in water and its heat stability was evaluated. It was observed that the sonicated-reconstituted whey protein solution shows heat stability even after storage. Again, this is an industrially important process. One could prepare heat-stable whey protein concentrates using ultrasonic technology, store and ship them to anywhere for reconstituting heat-stable dairy systems.

The ultrasonic processing to reduce viscosity has not only found to be useful for proteins, but starch system have also shown similar behaviour. It has been shown that heating of a starch slurry in aqueous solutions increase the viscosity significantly due to heat-induced gelation [92]. However, the physical forces generated during acoustic cavitation have disrupted such aggregation process leading to a significant reduction in solution viscosity. This is again an important process as the pasting properties of starch are important in some applications such as in the preparation of starch based confectionery. A detailed study by Zuo et al. [93] has shown that the pasting property of starch could be improved without affecting the molecular weight of the polymeric constituents in starch. In a separate study, Zuo et al. [93] have used high intensity low frequency ultrasound to study the surface damage caused by sonication. The focus of this study was to quantify the physical effects of cavitation on

the surface of starch granules. A strong correlation between the surface properties of starch granules and the number of pits generated up on the impact of cavitation-generated microjets was observed.

It could be clearly seen that ultrasonic technology offers a versatile avenue for synthesising a variety of functional materials. In addition, the physical effects of acoustic cavitation have been shown to be beneficial for processing food and dairy ingredients to increase their functionality.

References

1. C. Zhang, C. Li, J. Bai, J.Z. Wang, H. Li, Synthesis, characterization, and antibacterial activity of Cu NPs embedded electrospun composite nanofibers. Coll. Polym. Sci. **293**, 2525–2530 (2015)
2. Y. Liu, Y. Liu, N. Lioa, F. Cui, M. Park, H.Y. Kim, Fabrication and durable antibacterial properties of electrospun chitosan nanofibers with silver nanoparticles. Int. J. Biol. Macromol. **79**, 638–643 (2015)
3. H. Chen, D. Zhang, X. Zhou, J. Zhu, X.B. Chen, X.H. Zeng, Controllable construction of ordered porous SnO_2 nanostructures and their application in photocatalysis. Mater. Lett. **116**, 127–130 (2014)
4. V. Keller, P. Bernhardt, F. Garin, Photocatalytic oxidation of butyl acetate in vapor phase on TiO_2, Pt/TiO_2 and WO_3/TiO_2 catalysts. J. Catal. **215**, 129–138 (2003)
5. M. Ashokkumar, An overview on semiconductor particulate systems for photoproduction of hydrogen. Int. J. Hydrogen Energy **23**, 427–438 (1998)
6. V. Torchilin, M.M. Amiji (Eds), Handbook of Materials for Nanomedicine, Pan Stanford Series on Biomedical Nanotechnology, (2010)
7. C. Chen, C. Gao, M. Liu, S. Lu, C. Yu, S. Ma, J. Wang, G. Cui, Preparation and characterization of OSA/CS core-shell microgel: in vitro drug release and degradation properties. J. Biomater. Sci. Polym. Ed. **24**, 1127–1139 (2013)
8. S. Maiti, S. Mukherjee, R. Datta, Core-shell nano-biomaterials for controlled oral delivery and pharmacodynamic activity of glibenclamide. Int. J. Biol. Macromol. **70**, 20–25 (2014)
9. S.I.U. Madrid, U. Pal, K. Umapada, Y.S. Kang, J. Kim, H. Kwon, J. Kim, Fabrication of Fe_3O_4@mSiO_2 core-shell composite nanoparticles for drug delivery applications. Nanoscale Res. Lett. **10**, 1–8 (2015)
10. D.H. Bremner, Recent advances in organic-synthesis utilizing ultrasound. Ultrson. Sonochem. **1**, S119–S124 (1994)
11. A. Gedanken, Using sonochemistry for the fabrication of nanomaterials. Ultrson. Sonochem. **11**, 47–55 (2004)
12. I. Rosenthal, J.Z. Sostaric, P. Riesz, Sonodynamic therapy—a review of the synergistic effects of drugs and ultrasound. Ultrson. Sonochem. **11**, 349–363 (2004)
13. J.H. Bang, K.S. Suslick, Applications of ultrasound to the synthesis of nanostructured materials. Adv. Mater. **22**, 1039–1059 (2010)
14. B.G. Pollet, The use of ultrasound for the fabrication of fuel cell materials. Int. J. Hydrogen Energy **35**, 11986–12004 (2010)
15. T.J. Mason, Therapeutic ultrasound an overview. Ultrson. Sonochem. **18**, 847–852 (2011)
16. J. Chandrapala, C. Oliver, S. Kentish, M. Ashokkumar, Ultrasonics in food processing. Ultrson. Sonochem. **19**, 975–983 (2012)
17. F. Cavalieri, M. Zhou, M. Tortora, M. Ashokkumar, Methods of preparation of multifunctional microbubbles and their in vitro/in vivo assessment of stability, functional and structural properties. Curr. Pharm. Des. **18**, 2135–2151 (2012)

18. T. Harifi, M. Montazer, A review on textile sonoprocessing: a special focus on sonosynthesis of nanomaterials on textile substrates. Ultrson. Sonochem. **23**, 1–10 (2015)
19. G. Chatel, K.D.O. Vigier, F. Jerome, Sonochemistry: what potential for conversion of lignocellulosic biomass into platform chemicals? ChemSusChem **7**, 2774–2787 (2014)
20. T.J. Mason, D. Peters, *Practical Sonochemistry* (Woodhead Publishing, Cambridge, 2002)
21. L.A. Crum, T.J. Mason, J.L. Reisse, K.S. Suslick (eds.), Sonochemistry and Sonoluminescence. NATO ASI Series C: Mathematical and Physical Sciences, vol. 524, (Kluwer Academic Publishers, 1999)
22. G.V. Barbosa-Canovas, J. Weiss (eds.) Ultrasound Technologies for Food and Bioprocessing. Food Engineering Series. (Springer, 2011)
23. F.M Nowak, (2011) Sonochemistry: Theory, Reactions and Syntheses, and Applications. (Nova Science Publishers Inc., New York)
24. D. Chen, S.K. Sharma, A. Mudhoo (eds.), *Handbook on applications of ultrasound: sonochemistry for sustainability* (CRC Press, 2011)
25. P. Diodati, G. Giannini, L. Mirri, C. Petrillo, F. Sacchetti, Sonochemical production of a non-crystalline phase of palladium. Ultrson. Sonochem. **4**, 45–48 (1997)
26. K.S. Suslick, S.B. Choe, A.A. Cichowlas, M.W. Grinstaff, Sonochemical synthesis of amorphous iron. Nature **353**, 414–416 (1991)
27. K.S. Suslick, T. Hyeon, M. Fang, A.A. Cichowlas, in *Sonochemical preparation of nanostructured catalysts in Advances in Catalytic Nanostructured Materials*, ed. by W. Moser, (Academic Publishers, 1996), pp. 197–212
28. N.A. Dhas, A. Gedanken, Sonochemical preparation and properties of nanostructured palladium metallic clusters. J. Mater. Chem. **8**, 445–450 (1998)
29. Y. Koltypin, G. Katabi, X. Cao, R. Prozorov, A. Gedanken, Sonochemical preparation of amorphous nickel. J. Non-Cryst. Solids **201**, 159–162 (1996)
30. N.A. Dhas, C.P. Raj, A. Gedanken, Preparation of luminescent silicon nanoparticles: a novel sonochemical approach. Chem. Mater. **10**, 3278–3279 (1998)
31. M.M. Mdleleni, T. Heyon, K.S. Suslick, Sonochemical synthesis of nanostructured molybdenum sulphide. J. Am. Chem. Soc. **120**, 6189–6190 (1998)
32. A. Henglein, Contributions to various aspects of cavitation chemistry. Adv. Sonochem. **3**, 17–83 (1993)
33. K. Okitsu, S. Nagaoka, S. Tanabe, H. Matsumoto, Y. Mizukoshi, Y. Nagata sonochemical preparation of size-controlled palladium nanoparticles on alumina surface. Chem. Lett. 271–272. (1999)
34. K. Okitsu, H. Bandow, Y. Maeda, Sonochemical preparation of ultrafine palladium particles. Chem. Mater. **8**, 315–317 (1996)
35. K. Okitsu, M. Ashokkumar, F. Grieser, Sonochemical synthesis of gold nanoparticles in water: effects of ultrasound frequency. J. Phys. Chem. B **109**, 20673–20675 (2005)
36. R.A. Caruso, M. Ashokkumar, F. Grieser, Sonochemical formation of colloidal platinum. Colloids Surf. A **169**, 219–225 (2000)
37. M. Ashokkumar, F. Grieser, Sonochemical preparation of colloids, in *Encyclopaedia of Surface and Colloid Science*, ed. by A. Hubbard (Marcel Dekker, New York, 2002), pp. 4760–4774
38. R.A. Caruso, M. Ashokkumar, F. Grieser, Sonochemical formation of gold sols. Langmuir **18**, 7831–7836 (2002)
39. Y. He, K. Vinodgopal, M. Ashokkumar, F. Grieser, Sonochemical synthesis of ruthenium nanoparticles. Res. Chem. Intermed. **32**, 709–715 (2006)
40. K. Vinodgopal, Y. He, M. Ashokkumar, F. Grieser, Sonochemically prepared platinum-ruthenium bimetallic nanoparticles. J. Phys. Chem. B **110**, 3849–3852 (2006)
41. S. Anandan, F. Grieser, M. Ashokkumar, Sonochemical synthesis of Au-Ag core-shell bimetallic nanoparticles. J. Phys. Chem. C **112**, 15102–15105 (2008)
42. P.S.S. Kumar, A. Manivel, S. Anandan, M. Zhou, F. Grieser, M. Ashokkumar, Sonochemical synthesis and characterization of gold-ruthenium bimetallic nanoparticles. Coll. Surf. A Physicochem. Eng. Aspects **356**, 140–144 (2010)

43. K. Vinodgopal, B. Neppolian, I.V. Lightcap, F. Grieser, M. Ashokkumar, P.V. Kamat, Sonolytic design of graphene-Au nanocomposites. Simultaneous and sequential reduction of graphene oxide and Au(III). J. Phys. Chem. Lett. **1**, 1987–1993 (2010)
44. K. Vinodgopal, B. Neppolian, N. Salleh, I.V. Lightcap, F. Grieser, M. Ashokkumar, T.T. Ding, P.V. Kamat, Duel-frequency ultrasound for designing two dimensional catalyst surface: reduced graphene oxide-Pt composite. Coll. Surf. A Physicochem. Eng. Aspects **409**, 81–87 (2012)
45. B. Neppolian, V. Saez, J.-G. Garcia, F. Grieser, R. Gomez, M. Ashokkumar, Sonochemical synthesis of graphene oxide supported Pt–Pd alloy nanocrystals as efficient electrocatalysts for methanol oxidation. J. Solid State Electrochem. **18**, 3163–3171 (2014)
46. S. Anandan, S.-D. Oh, M. Yoon, M. Ashokkumar, Photoluminescence properties of sonochemically synthesized gold nanoparticles for DNA biosensing. Spectrochimica Acta Part A Mol. Biomol. Spectrosc. **76**, 191–196 (2010)
47. M. Ni, M.K.H. Leung, Y.C. Denise, K. Sumathy, A review and recent developments in photocatalytic water-splitting using TiO_2 for hydrogen production. Renew. Sustain. Energy. Rev. **11**, 401–425 (2007)
48. U.I. Gaya, A.H. Abdullah, Heterogeneous photocatalytic degradation of organic contaminants over titanium dioxide: a review of fundamentals, progress and problems. J. Photochem. Photobiol. C Photochem. Rev **9**, 1–12 (2008)
49. S. Lee, S.-J. Park, TiO_2 photocatalyst for water treatment applications. J. Ind. Eng. Chem. **19**, 1761–1769 (2013)
50. S.S. Watson, D. Beydoun, J.A. Schott, R. Amal, The effect of preparation method on the photoactivity of crystalline titanium dioxide particles. Chem. Eng. J. **95**, 213–220 (2003)
51. S. Sakulkhaemaruethai, Y. Suzuki, S. Yoshikawa, Surfactant-assisted preparation and characterization of mesoporous titania nanocrystals—effect of various processing conditions. J. Ceramic Soc. Jpn. **112**, 547–552 (2004)
52. M.S. Lee, G.D. Lee, C.S. Ju, S.S. Hong, Preparations of nanosized TiO_2 in reverse microemulsion and their photocatalytic activity. Sol. Energy. Mater. Sol. Cells **88**, 389–401 (2005)
53. B. Mukherjee, C. Karthik, N. Ravishankar, Hybrid sol-gel combustion synthesis of nanoporous anatase. J. Phys. Chem. C **113**, 18204–18211 (2009)
54. G. Zhang, F. Teng, Y. Wang, P. Zhang, C. Gong, L. Chen, C. Zhao, E. Xie, Preparation of carbon-TiO_2 nanocomposites by a hydrothermal method and their enhanced photocatalytic activity. RSC Adv. **3**, 24644–24649 (2013)
55. C.W. Oh, G.D. Lee, S.S. Park, C.S. Ju, S.S. Hong, Synthesis of nanosized TiO_2 particles via ultrasonic irradiation and their photocatalytic activity. Reaction Kin. Catal. Lett. **85**, 261–268 (2005)
56. A. Nakaruk, G. Kavei, C.C. Sorrell, Synthesis of mixed-phase titania films by low-temperature ultrasonic spray pyrolysis. Mater. Lett. **64**, 1365–1368 (2010)
57. J. Guo, S. Zhu, Z. Chen, Y. Li, Z. Yu, Q. Liu, J. Li, C. Feng, D. Zhang, Sonochemical synthesis of TiO_2 nanoparticles on graphene for use as photocatalyst. Ultrason. Sonochem. **18**, 1082–1090 (2011)
58. I. Hernandez-Perez, A.M. Maubert, L. Rendon, P. Santiago, H. Herrera-Hernandez, L.D.B. Arceo, V.G. Febles, E.P. Gonzalez, L. Gonzalez-Reyes, Ultrasonic synthesis: structural, optical and electrical correlation of TiO_2 nanoparticles. Int. J. Electrochem. Sci. **7**, 8832–8847 (2012)
59. S. Anandan, G.-J. Lee, C.-K. Yang, M. Ashokkumar, J.J. Wu, Sonochemical synthesis of Bi2CuO4 nanoparticles for catalytic degradation of nonylphenol ethoxylate. Chem. Eng. J. **183**, 46–52 (2012)
60. M. Zhou, B. Babgi, S. Gupta, F. Cavalieri, Y. Alghamdi, M. Aksu, M. Ashokkumar, Ultrasonic fabrication of TiO_2/chitosan hybrid nanoporous microspheres with antimicrobial properties. RSC Adv. **5**, 20265–20269 (2015)
61. B.M. Teo, S.W. Prescott, M. Ashokkumar, F. Grieser, Ultrasound initiated miniemulsion polymerization of methacrylate monomers. Ultrason. Sonochem. **15**, 89–94 (2008)
62. M. Bradley, F. Grieser, J. Coll. Interface Sci. **251**, 78–84 (2002)

63. G.J. Price, Recent developments in sonochemical polymerisation. Ultrason. Sonochem. **10**, 277–283 (2003)
64. K.S. Suslick, G.J. Price, Applications of ultrasound to materials chemistry. Ann. Rev. Mater. Sci. **29**, 295–326 (1999)
65. B. Teo, M. Ashokkumar, F. Grieser, Microemulsion polymerisation via high frequency ultrasound irradiation. J. Phys. Chem. C **112**, 5265–5267 (2008)
66. B.M. Teo, M. Ashokkumar, F. Grieser, Sonochemical polymerisation of miniemulsions in organic liquids/water mixtures. Phys. Chem. Chem. Phys. **13**, 4095–4102 (2011)
67. B.M. Teo, S.W. Prescott, G.J. Price, F. Grieser, M. Ashokkumar, Synthesis of temperature responsive poly(N-isopropylacrylamide) using ultrasound irradiation. J. Phys. Chem. B **114**, 3178–3184 (2010)
68. B.M. Teo, F. Chen, T.A. Hatton, F. Grieser, M. Ashokkumar, A novel one-pot synthesis of magnetite latex nanoparticles by ultrasound irradiation. Langmuir **25**, 2593–2595 (2009)
69. M. Bradley, M. Ashokkumar, F. Grieser, Sonochemical production of fluorescent and phosphorescent latex particles. J. Am. Chem. Soc. **125**, 525–529 (2003)
70. K. Nakabayashi, F. Amemiya, T. Fuchigami, K. Machida, S. Takeda, K. Tamamitsu, M. Atobe, Highly clear and transparent nanoemulsion preparation under surfactant-free conditions using tandem acoustic emulsification. Chem. Commun. **47**, 5765–5767 (2011)
71. K. Nakabayashi, M. Kojima, S. Inagi, Y. Hirai, M. Atobe, Size-controlled synthesis of polymer nanoparticles with tandem acoustic emulsification followed by soap-free emulsion polymerization. ACS Macro Lett. **2**, 482–484 (2013)
72. M.W. Grinstaff, K.S. Suslick, Proteinaceous microspheres. ACS Symp. Ser. **493**, 218–226 (1992)
73. F.J.J. Toublan, S. Boppart, K.S. Suslick, Tumor targeting by surface-modified protein microspheres. J. Am. Chem. Soc. **128**, 3472–3473 (2006)
74. F. Cavalieri, M. Ashokkumar, F. Grieser, F. Caruso, Ultrasonic synthesis of stable, functional lysozyme microbubbles. Langmuir **24**, 10078–10083 (2008)
75. A. Gedanken, Preparation and properties of proteinaceous microspheres made sonochemically. Chem. Europ. J **14**, 3840–3853 (2008)
76. F. Cavalieri, M. Zhou, F. Caruso, M. Ashokkumar, One-pot ultrasonic synthesis of multifunctional microbubbbles and microcapsules using synthetic thiolated macromolecules. Chem. Commun. **47**, 4096–4098 (2011)
77. F. Cavalieri, L. Micheli, S. Kaliappan, B.M. Teo, M. Zhou, G. Palleschi, M. Ashokkumar, Antimicrobial and biosensing ultrasound-responsive lysozyme-shelled microbubbles. ACS Appl. Mater. Interface. **5**, 464–471 (2013)
78. S. Melino, M. Zhou, M. Tortora, M. Paci, F. Cavalieri, M. Ashokkumar, Molecular properties of lysozyme-microbubbles: towards the protein and nucleic acid delivery. Amino Acids **43**, 885–896 (2012)
79. M. Zhou, F. Cavalieri, F. Caruso, M. Ashokkumar, Confinement of acoustic cavitation for the synthesis of protein-shelled nanobubbles for diagnostics and nucleic acid delivery. ACS Macro Lett. **1**, 853–856 (2012)
80. F. Chemat, Zill-e-Huma, M.K. Khan, Applications of ultrasound in food technology: processing, preservation and extraction. Ultrason. Sonochem. **18**, 813–835 (2011)
81. Y. Tao, D.-W. Sun, Enhancement of food processes by ultrasound: a review. Crit. Rev. Food Sci. Nutr. **55**, 570–594 (2015)
82. A. Shanmugam, M. Ashokkumar, Ultrasonic preparation of stable flax seed oil emulsions in dairy systems—physicochemical characterization. Food Hydrocolloids **39**, 151–162 (2014)
83. A. Shanmugam, M. Ashokkumar, Characterization of ultrasonically prepared flaxseed oil enriched beverage/carrot juice emulsions and process-induced changes to the functional properties of carrot juice. Food Bioprocess Technol. **8**, 1258–1266 (2015)
84. M.F. Ertugay, M. Sengul, M. Sengul, Effect of ultrasound treatment on milk homogenisation and particle size distribution of fat. Turk. J. Vet. Anim. Sci. **28**, 303–308 (2004)

85. J. Chandrapala, B. Zisu, S. Kentish, M. Ashokkumar, The effects of high-intensity ultrasound on the structural and functional properties of α-Lactalbumin, β-Lactoglobulin and their mixtures. Food Res. Int. **48**, 940–943 (2012)
86. A. Shanmugam, J. Chandrapala, M. Ashokkumar, The effect of ultrasound on the physical and functional properties of skim milk. Innov. Food Sci. Emerg Technol. **16**, 251–258 (2012)
87. M. Ashokkumar, J. Lee, B. Zisu, R. Bhaskaracharya, M. Palmer, S. Kentish, Sonication increases the heat stability of whey proteins. J. Dairy Sci. **92**, 5353–5356 (2009)
88. J. Chandrapala, B. Zisu, M. Palmer, S. Kentish, M. Ashokkumar, Effects of ultrasound on the thermal and structural characteristics of proteins in reconstituted whey protein concentrate. Ultrason. Sonochem. **18**, 951–957 (2011)
89. B. Zisu, J. Lee, J. Chandrapala, R. Bhaskaracharya, M. Palmer, S. Kentish, M. Ashokkumar, Effect of ultrasound on the physical and functional properties of reconstituted whey protein powders. J. Dairy Res. **78**, 226–232 (2011)
90. B. Zisu, R. Bhaskaracharya, S. Kentish, M. Ashokkumar, Ultrasonic processing of dairy systems in large scale reactors. Ultrason. Sonochem. **17**, 1075–1081 (2010)
91. J. Chandrapala, B. Zisu, M. Palmer, S.E. Kentish, M. Ashokkumar, Sonication of milk protein solutions prior to spray drying and the subsequent effects on powders during storage. J. Food Eng. **141**, 122–127 (2014)
92. J. Zuo, K. Knoerzer, R. Mawson, S. Kentish, M. Ashokkumar, The pasting properties of waxy rice starch suspensions. Ultrason. Sonochem. **16**, 462–468 (2009)
93. Y.Y.J. Zuo, P. Hebraud, Y. Hemar, M. Ashokkumar, Quantification of high-power ultrasound induced damage on potato starch granules using light microscopy. Ultrason. Sonochem. **19**, 421–426 (2012)

http://www.springer.com/978-3-319-28972-4

Ultrasonic Synthesis of Functional Materials

Ashokkumar, M.

2016, IX, 42 p. 21 illus., Softcover
ISBN: 978-3-319-28972-4